Academic Science Journal (ASJ)
Vol. 4, No. 3, July 2026, pp. 23~ 32
DOI: 10.24237/04.03.524

Synthesis and Characterization of 2-amino-5- chloro benzophenoxime and Using as Corrosion Inhibitor for low-carbon steel (SS41) alloy

Ali Adnan Fadhel Al-Azzawi [1], Ahmed Najem Abd [2], Luma Salman Abd[2]
[1]Department of Diyala Education, Ministry of Education, Diyala, Iraq.
[2]Department of Chemistry, College of Science, Diyala University, Diyala, Iraq.

Article Info

Article history:

Received 19, 10, 2024
Revised 08, 12, 2024
Accepted 30, 02, 2025
Published 30, 07, 2026

Keywords:

Corrosion,
Inhibitor,
Benzophenoxime,
low-carbon steel,
acidic solution.

ABSTRACT

Inhibition is a key approach for reducing corrosion in low-carbon steel alloys. In this investigation, In order to maintain a low-carbon steel (SS41) alloy at (25, 35, 45, and 55) °C, an organic molecule (2-amino-5-chloro benzophenoxime) was created and used. A synthetic chemical was used at six concentrations (50, 100, 150, 200, 250, and 300 ppm). In corrosion tests, inhibited surface analysis, and other thermodynamic methods were utilized to analyze the inhibition process. FT-IR, ^{1}HNMR, and ^{13}CNMR were employed to characterize the produced component. The corrosion test (weight loss) revealed a high inhibition efficiency (IE %). 2-amino-5-chloro benzophenoxime yielded 87.77% at 55 °C and 300 ppm in 0.5 M H_2SO_4. Three adsorption isotherms were used to investigate inhibitor adsorption. Adsorption isotherms include the Langmuir, Freundlich, and Temkin isotherms. The standard free energy of adsorption (Heat of Adsorption, $\Delta G^{o}ads$) was calculated using the equilibrium constant values obtained from the Langmuir equation in order to determine the type of adsorption (physical, chemical, or mixed). This research determined the adsorption to be physical. SEM examination of the inhibited surface revealed that the chemical molecules were adsorbing on the low-carbon steel (SS41) surface, causing inhibition. Surface roughness was detected using AFM images.

Corresponding Author:

Ali Anan Fadhel Al-Azzawi
Department of Diyala Education , Ministry of Education,
Al-Khalis City, Diyala Governorate, Iraq.
Email: aliadnan1989ali@gmail.com

1. INTRODUCTION

Corrosion is a damaging process that occurs when metals come into touch with their surroundings [1]. It should be noted that the term "corrosion" refers to metal deterioration caused by external sources. The primary focus of this research will be metal corrosion. However, other materials, such as plastic, wood, concrete, ceramics, and composites, can degrade under certain conditions. The oxidation of iron and steel by carbon is known as "rusting." The ferric oxide is hydrated, and the rust layer is a reddish brown color. As a result, steel corrodes and rusts, whereas aluminum, copper, and zinc corrode but never rust [2][3].Corrosion inhibitors were developed to be a more effective and convenient method of controlling corrosion. Chemical inhibitors are used to slow down the rate of corrosion processes. Corrosion inhibitors are used in a variety of industries, including oil and gas, the chemical industry, production, refineries, heavy industry, water treatment [4]. Inhibitors are often chemical or inorganic substances that dissolve in water. Carbonates, chromates, nitrites, silicates, and phosphates are some of the most potent inorganic inhibitors. Organic inhibitors include amines, nitrogen compounds, thioethers, thiol alcohols, thiamides, thioureas, and hydrazine. Chromates and zinc salts are no longer widely utilized due to their toxicity, and have been mostly supplanted with organic inhibitors. Organic inhibitors are the initial line of defense, hence a large number of compounds (ideally organic) are utilized in modest amounts. Any organic compounds efficiency is defined by its capacity to be absorbed on metal surfaces.

An organic inhibitor containing donor groups promotes inhibition, and vice versa. During metal-inhibitor interaction, the negatively charged metal surface attracts positively charged inhibitor molecules due to the electrostatic force of attraction. The grade of the metal influences the bond strength and substituent qualities on the original molecular structure, which in turn influence the parameters of the metal-inhibitor interaction. The inhibitory molecules are meant to shield the metal substrate from corrosion ions, hence preventing corrosion [6].Oximes (R1R2C=N-OH) are a prominent class of hydroxylamines (R1R2NOH), where R2 is either hydrogen (forming aldoxime) or another aromatic group (forming ketoximes), and R1 is an organic side chain (e.g., alkyl, cycloalkyl, or aromatic moiety)[7]. In addition to being useful as a convenient protective group in synthetic chemical applications, oxime functional groups can be transformed into important groups including carbonyl, amino, nitro, and cyano functionalities [8].The classic and extensively utilized dynamic covalent reaction, oxime, comprises the general acid-catalyzed attack of α-nucleophile (aminooxy) to carbonyl carbon, followed by water elimination to generate the oxime product [9].

2. METHOD

2.1. Setting Up the Corrosion Media

A 0.5 M solution of H_2SO_4 was one of the corrosion media that were studied. After making this medium with distilled water, it was added to 500 mL flasks that held different concentrations of the synthesized oxime.

2.2. low-carbon steel (SS41) Preparation

This study investigated corrosion and inhibition in acidic settings using low-carbon steel (SS41). Table 1 displays the chemical composition of low-carbon steel as determined by Foundry Master X_{pert} in the Ministry of Planning's Centralized Device for Standardization and Quality Control. Initially, low-carbon steel (SS41) specimens were created to investigate the corrosion test (loss weigh). Cutting the specimen is thought to be a crucial component of corrosion resistance, and a consistent surface is essential. With a hole drilled on one side for easy suspension in the corroding solution, square specimens measuring 3 cm by 3 cm by 1 cm were cut into the final specimen shape using an electrical saw. To create a smooth, scratch-free surface, the specimens were then ground in the following order using paper: 220, 400, 600, 800, 1000, 1500, and 2000. The samples were polished with a suspension of alumina. Following that, distilled water was used to rinse the samples. The polished samples were cleaned with acetone, dried, and put in a plastic container. The samples' dimensions were measured with an electronic venire, and their weight was determined with a four-digit electronic balance[10].

Table1. Composition of low-carbon alloy (SS41)

Composition (WT%)							
C	% 0.153	Ni	% 0.0202	W	% 0.0208	Bi	< % 0.0015
Si	% 0.0924	Al	% 0.0167	Pb	< % 0.0010	As	< % 0.0005
Mn	% 0.236	Co	< % 0.0010	Sn	< % 0.0010	Se	< % 0.0010
P	< % 0.0005	Cu	% 0.0066	B	< % 0.0005	Sb	% 0.0074
S	< % 0.0010	Nb	% 0.0044	Ca	< % 0.0005	Ta	% 0.0094
Cr	% 0.284	Ti	< % 0.0005	Zr	< % 0.0010	Fe	% 99.1
Mo	% 0.0033	V	% 0.0021	Zn	% 0.0019		

2.3. Synthesis of 2-amino-5- chloro benzophenoxime

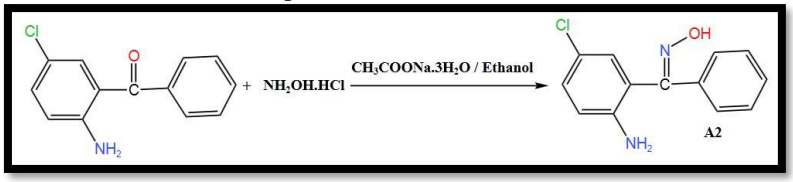

Scheme 1. Synthesis of 2-amino-5- chloro benzophenoxime

At ambient temperature, a solution of 2-amino-5-chlorobenzophenone (0.5g, 0.0037mol) in ethanol (20ml) was mixed with hydroxyl amine hydrochloride (0.52g, 0.0074mol) and sodium acetate trihydrate (1.02g, 0.0074mole) in distilled water (7ml). Following the additions, the mixture was placed in a 100ml round-bottom flask equipped with a magnetic stirrer and refluxed for 15 hours at 80 degrees Celsius (TLC-monitored; hexane:ethyl acetate ratio, 3:1). After cooling the combination in an ice bath for 1 hour, a yellowish white precipitate was filtered and recrystallized from ethanol, yielding (2-amino-5- chloro benzophenoxime). Table 2 provides physical information about the created chemical.

Table 2. Physical properties of 2-amino-5- chloro benzophenoxime

Melting Point	Color	Molecular Formula	Yield / %
>300 ℃	yellowish white	$C_{13}H_{11}ClN_2O$	64%

3. RESULTS AND DISCUSSION

3.1. Characterization of 2-amino-5- chloro benzophenoxime

The substance was produced by reacting 2-amino-5-chloro benzophenone with $NH_2OH.HCl$ and $CH_3COONa.3H_2O$, resulting in the production of a novel molecule detected by TLC. The FT-IR spectrum of the compound in Figure 1 shows different bands of absorption (KBr, cm^{-1}): stretch (3445) for the OH group, stretch (3226-3366) for the aliphatic NH2 group, stretch (3060) for aromatic CH, stretch (1625) for the C=N group (the ketone carbonyl group disappears), stretch (1489 and 1569) for C=C aromatic, stretching (925) for N-O, and stretch (778) for C-Cl. The ^{1}HNMR spectra of the compound in Figure 2 revealed the following chemical shifts (DMSO-d_6 ppm): 11.62 (S, 1H) for the OH group, 6.8 to 7.4 (m, 8H) for Ar-H, and signals 2.5 and 3.3 (S, 2H) for the NH_2 group. The ^{13}C-NMR spectra of the molecule in Figure 3 revealed the following signals (DMSO-d6, ppm): (153) for C=N and (117.2 to 145.2) for the aromatic ring.

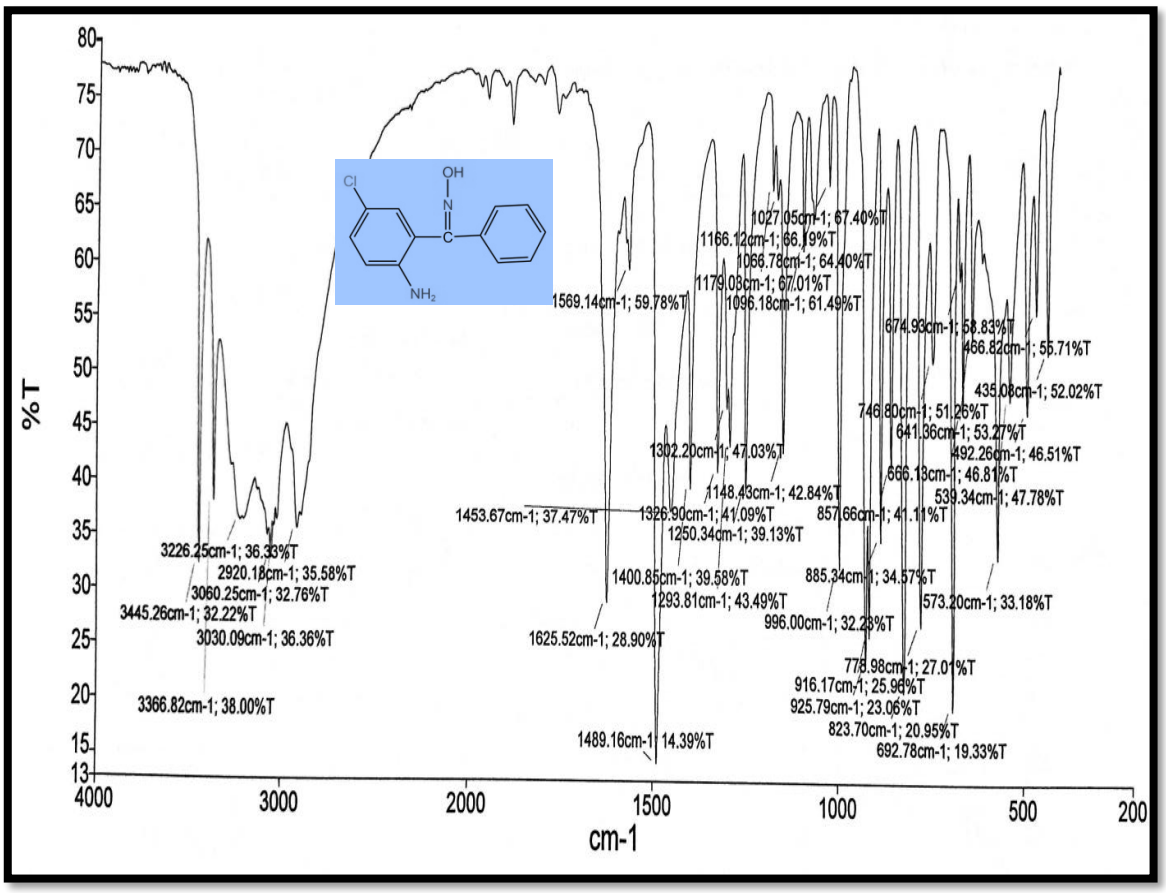

Figure 1. FT-IR spectrum

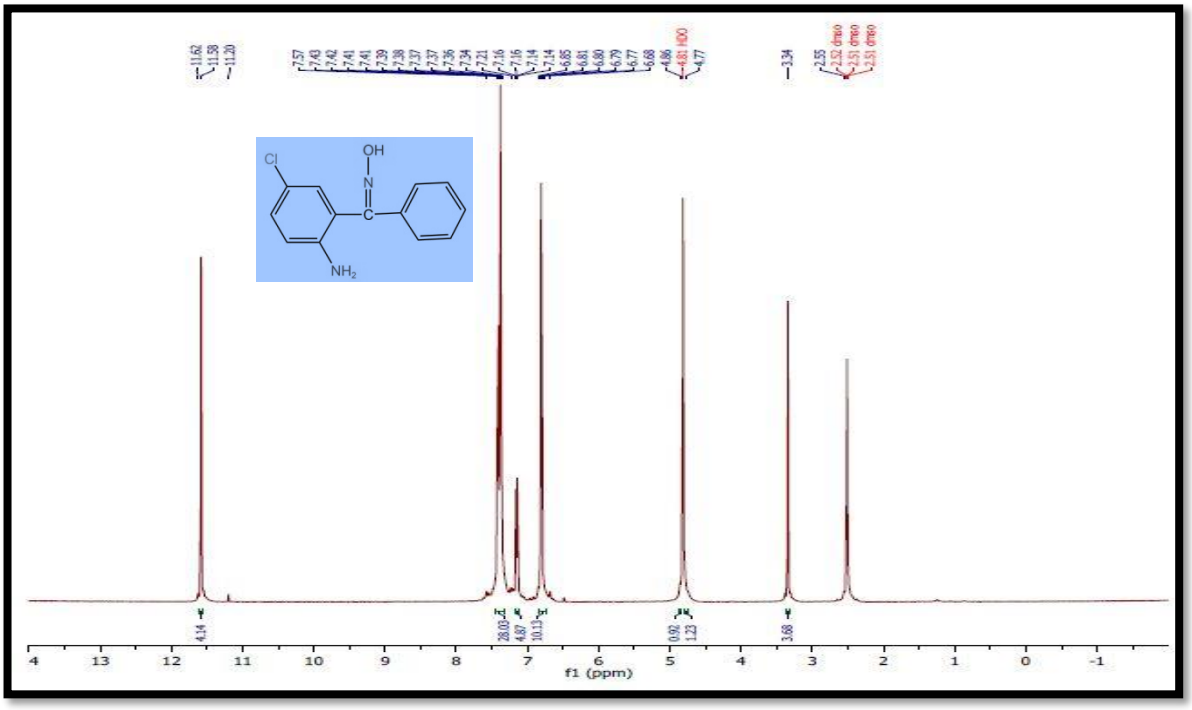

Figure 2. [1]HNMR spectrum

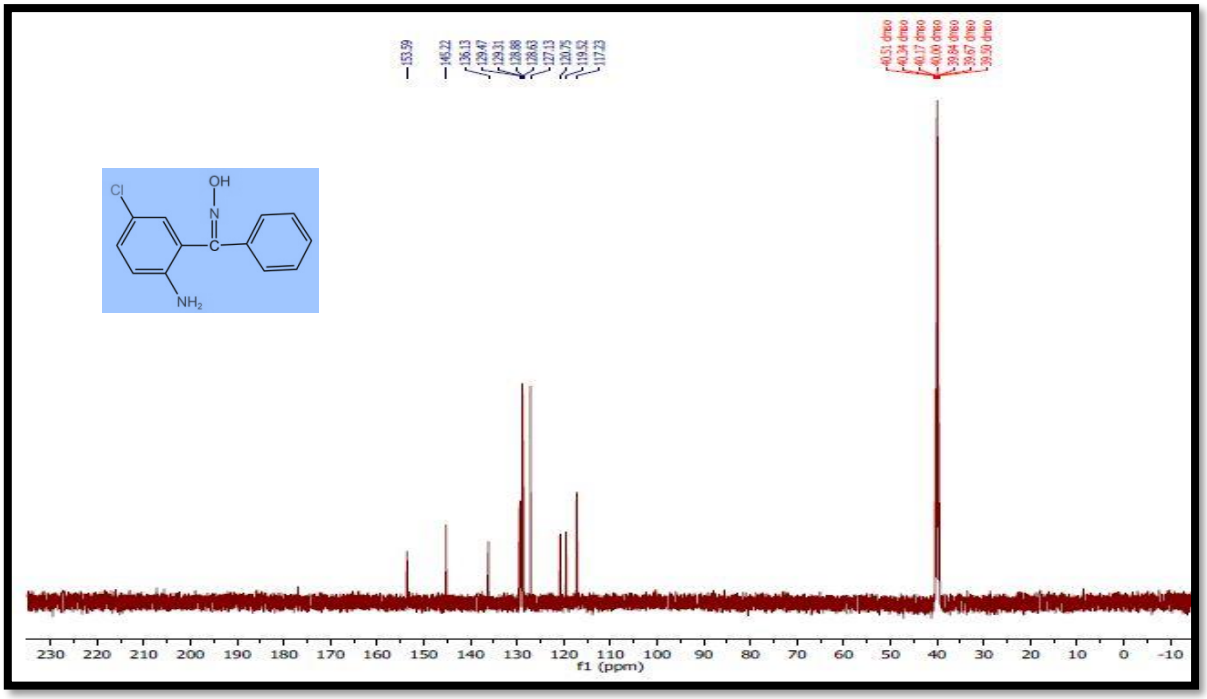

Figure 3. [13]CNMR spectrum

3.2. Weight loss method

For approximately three hours, when diving at (25, 35, 45, and 55) °C, the weight loss measurement of low-carbon steel (SS41) corrosion was examined in the presence and absence of various concentrations of 2-amino-5-chloro benzophenoxime in 0.5 M H2SO4. The following formula [11] was used to get the corrosion rate (CR):

$$\text{(gmd) CR correlation} = \Delta W/W \times t \quad \ldots\ldots\ldots(1)$$

The efficiency ratio is computed using (CR) corrosion rate, (ΔW) weight loss in grams, (A) sample area in (t), and m2 immersion duration in days. Corrosion rates are measured in g/m2 day and represented by (gmd). Damping with the following equation [12]:

$$\%IE = \frac{\text{CRuninhibit}\_\text{CRinhibit}}{\text{CRuninhibit}} \times 100 \ldots\ldots\ldots(2)$$

The rate and potency of damping was assessed under various implementation conditions, including temperature and concentration, and the results were compiled in Table 3, which explains why the rate of corrosion increases with temperature and decreases with increasing inhibitor concentration. Where (% IE) is the inhibition efficiency, and (CRuninhibit) and (CRinhibit) are the corrosion rates in the absence and presence of different inhibitory concentrations. The efficiency of inhibition rises with temperature and the concentration of the inhibitor.

Table 3. The impact of temperature on the rate of corrosion, the effectiveness of inhibition, and the surface coverage of low-carbon steel SS41 in 0.5M H2SO4 both with and without 2-amino-5-chloro benzophenoxime.

Time (3 hour)				
C_{inh} (ppm)	Temperature(°C)	C_R (gmd)	θ(surface coverage)	IE%
Blank	25	151.409	0	0
	35	346.640	0	0
	45	572.311	0	0
	55	736.665	0	0
50	25	67.301	0.5555	55.55
	35	137.859	0.6023	60.23
	45	186.402	0.6743	67.43
	55	209.287	0.7159	71.59
100	25	61.109	0.5964	59.64
	35	122.260	0.6473	64.73
	45	152.006	0.7344	73.44
	55	169.786	0.7695	76.95
150	25	56.264	0.6284	62.84
	35	110.682	0.6807	68.07
	45	128.140	0.7761	77.61
	55	144.534	0.8038	80.38
200	25	49.980	0.6699	66.99
	35	98.827	0.7149	71.49
	45	98.911	0.8278	82.78
	55	102.470	0.8609	86.09
250	25	44.605	0.7054	70.54
	35	88.671	0.7442	74.42
	45	90.184	0.8424	84.24
	55	95.950	0.8700	87
300	25	39.896	0.7365	73.65
	35	80.074	0.7690	76.90
	45	86.852	0.8482	84.82
	55	90.108	0.8777	87.77

3.3. Impact of inhibitory concentration on low-carbon steel (SS41) corrosion

Table (3) illustrates how different concentrations of 2-amino-5-chlorobenzophenoxime in (0.5M H_2SO_4) at room temperature impede the efficiency of low-carbon steel (SS41). As the concentration of the inhibitor increased, the corrosion rate evidently dropped. As the inhibitor concentration rises, this trend is brought about by the retarder's enhanced adsorption and coverage on the low-carbon steel (SS41) surface suggested improved 2-amino-5-chloro benzophenoxime inhibitory performance with a high ability to bind to the inhibitor on the surface of low-carbon steel (SS41) [14]. The adsorption behavior of the adsorptive substance on the roof of the alloy must be understood in order to comprehend the anti-corrosion process. Information about the way inhibitor particles interact with a metal surface can be obtained from isotropic. Based on weight loss, the grade of surface coverage (Θ =IE/100) for various inhibitory dosages was calculated. To investigate the kinematics of adsorption on metal surfaces, three models are put forth. To find the Langmuir absorption temperature, utilize equation (3).

$$\frac{c}{\theta} = \frac{1}{Kads} + c \quad \text{.....(3)}$$

$$\theta = K_{ads}\, C^{\wedge 1/n} \quad \text{.....(4)}$$

The grade of surface coverage (Θ), concentration inhibitor (C), adsorptive static equilibrium (kads), and molecular interaction parameters (is) are used.

$$K_{ads} = \frac{1}{55.5} exp^{\frac{\Delta G^o}{RT}} \quad \text{.....(5)}$$

where (55.5) is the water concentration in solution given in M, and $\Delta G^{o}ads$ is the standard adsorption free energy (kJ mol^{-1}). Equation (6) was used to test the adsorption isotherm and to determine the Freundlich adsorption temperature.

$$Ln\theta = \ln K_f + n \ln C \ldots\ldots\ldots\ldots\ldots\ldots (6)$$

Temkin isothermal adsorption, as specified in equation (7), was utilized to characterize the adsorption of surface adsorption inhibitors on low-carbon steel (SS41).

$$\exp(-2a\theta) = k_{ads}\, C \ldots\ldots\ldots\ldots\ldots (7)$$

Equations (3), (6), (7) it can be drawn as shown in Figure 4, 5, 6.

Table 4 provides the kinematic data. The method of Langmuir isotherm adsorption yielded the highest correlation values (R^2), as Table 4 illustrates. The most effective retarder had negative values ($\Delta G°_{ads}$) and a higher acid concentration, which showed a drop in efficiency damping and an increase in acid concentration as a result of adsorption. This suggests a substantial surface adsorption of the metal. A usual rule of thumb was that values of ($\Delta G°_{ads}$) greater than (-20 in $KJmol^{-1}$) indicated physical adsorption, whereas values greater than (-40 $KJmol^{-1}$) indicated chemical absorption. The physisorption mechanism was corroborated by the experiment, which showed (ΔG^{o}_{ads}) values that had a negative value less than (20 $KJmol^{-1}$) [13][14].

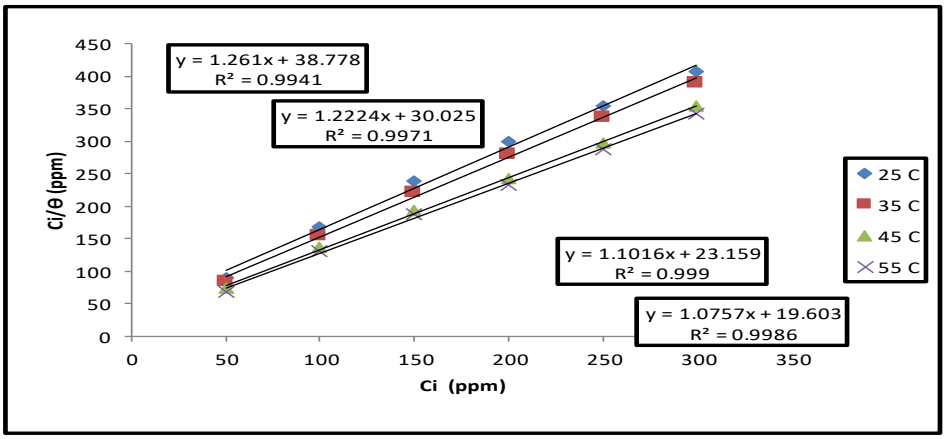

Figure 4. Langmuir adsorption isotherm of (2-amino-5- chloro benzophenoxime) for low-carbon steel (SS41) corrosion in (0.5 M H_2SO_4).

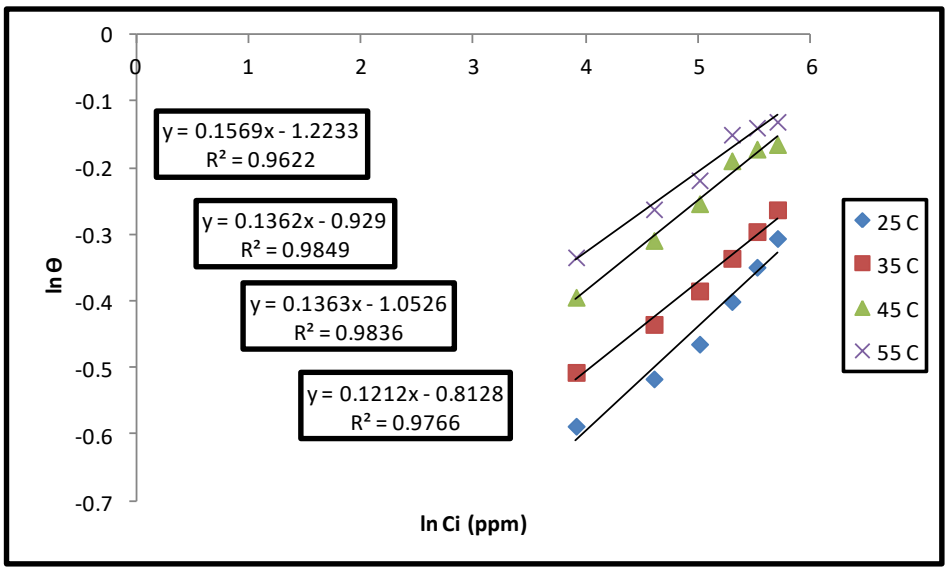

Figure 5. Isotherm Freundlich adsorption of (2-amino-5- chloro benzophenoxime)for low-carbon steel (SS41) corrosion in (0.5M H_2SO_4)

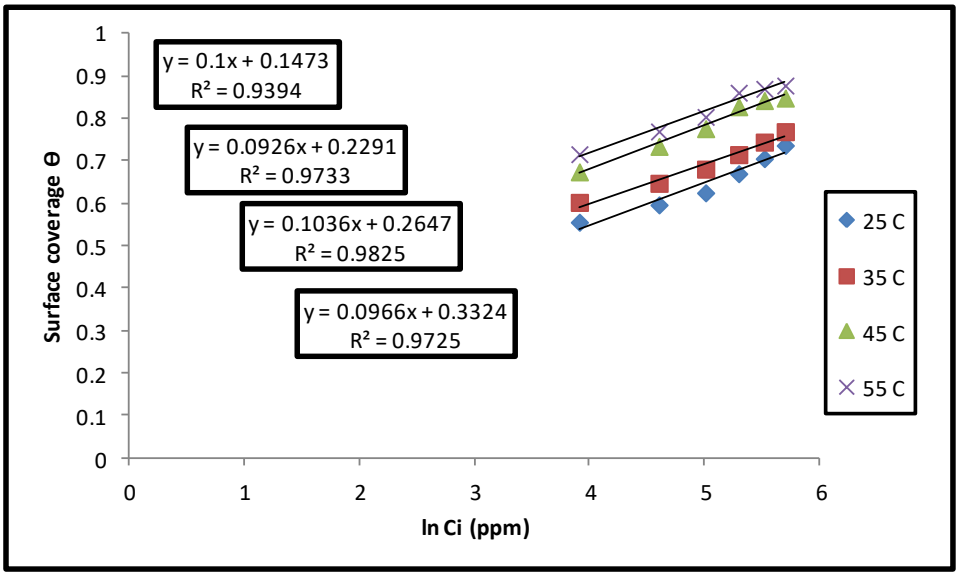

Figure 6. Timken adsorption isotherm of (2-amino-5- chloro benzophenoxime) for low-carbon steel (SS41) corrosion in (0.5M H_2SO_4).

Table 4. Parameters of the adsorption of low-carbon steel (SS41) corrosion in (0.5MH_2SO_4)

T(K)	Langmuir isothermal adsorption			Freundlich adsorption isotherms			Timken adsorption isotherm		
	K_L (L/mg)	ΔG°ads (kJ/mol)	R^2	K_F (L/mg)	N	R^2	K_T (L/mg)	A	R^2
0.0257	- 2.4788	0.9941	0.0257	0.2943	0.1569	0.9622	0.1000	1.1587	0.9394
0.0333	- 1.5735	0.9971	0.0333	0.3490	0.1363	0.9836	0.0926	1.2575	0.9733
0.0431	- 2.3069	0.999	0.0431	0.3949	0.1362	0.9849	0.1036	1.3030	0.9825
0.0510	- 2.8386	0.9986	0.0510	0.4436	0.1212	0.9766	0.0966	1.3943	0.9725

3.4. Inspection of the surface by (AFM)

Atomic force microscopy characterization (AFM) is a strong approach for examining surface morphology at the nano- to microscale, and it is being employed as a novel alternative for studying the effect of inhibitors on the onset and progression of corrosion on metals[15][16]. Figure 7 depicts 2D and 3D images of the polished surface of low-carbon steel (SS41), which has a root mean square height (Sq) of 49.09nm and an arithmetic mean height (Sa) of 40.99nm due to air corrosion during sample transport for inspection. Figure 8 depicts a corroded surface in H_2SO_4 medium for low-carbon steel (SS41), with a root mean square height (Sq) of 279.6nm and an arithmetic mean height (Sa) of 226.9nm produced by corrosion and rust. Figure 9 depicts an AFM test of the inhibited surface in 0.5 M H2SO4 medium containing 2-amino-5-chloro benzophenoxime for low-carbon steel (SS41), with a root mean square height (Sq) of 1100nm and arithmetic mean height (Sa) of 894.4nm. Caused by the molecular structure that has been adsorbed on the surface.

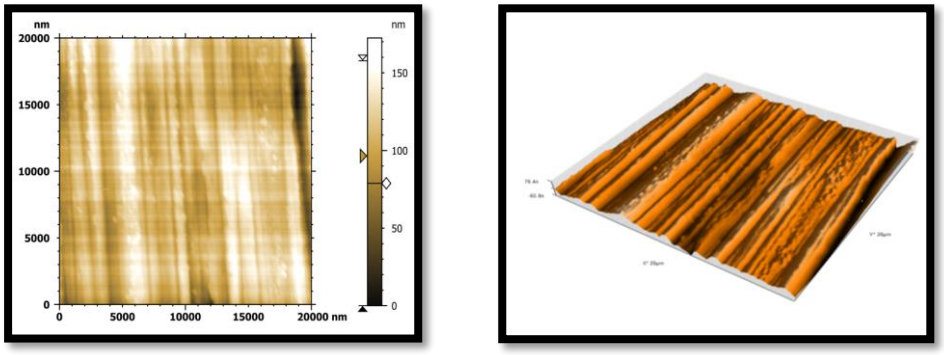

Figure 7. Shows 2D and 3D images of AFM for a polished low-carbon steel (SS41) surface.

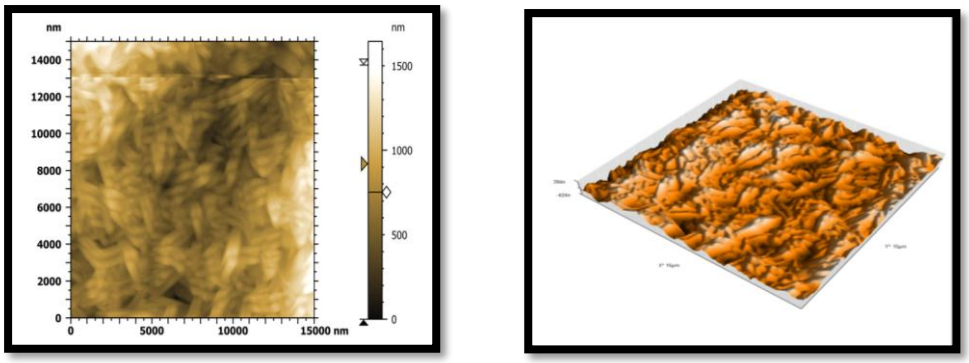

Figure 8. Shows 2D and 3D images of an AFM low-carbon steel (SS41) surface immersed in 0.5M H_2SO_4.

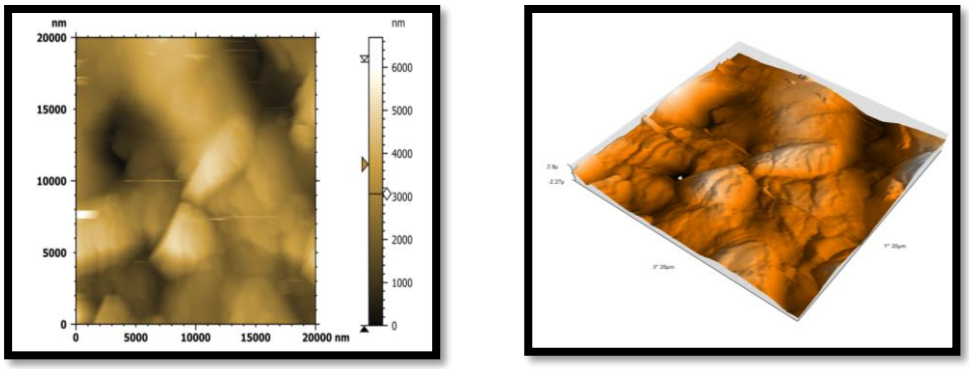

Figure 9. Shows 2D and 3D images of an AFM low-carbon steel (SS41) surface immersed in (0.5M H_2SO_4) with 300 ppm of 2-amino-5- chloro benzophenoxime.

3.5. Scanning electron microscope (SEM)

The microstructure of low-carbon steel (SS41) was examined using a scanning electron microscope (SEM). Figure 10 depicts a scanning electron microscopy (SEM) image of a low-carbon steel (SS41) specimen before immersion in a corrosion solution. Figure 11 depicts low-carbon steel (SS41) after three hours of immersion in a corrosion solution (0.5 M H_2SO_4). Figure 12 depicts low-carbon steel (SS41) immersed in an acid solution (0.5 M H_2SO_4) with the organic inhibitor 2-amino-5-chloro benzophenoxime at optimal concentration (300 PPM) and temperature (55 ℃) based on IE% values.

.

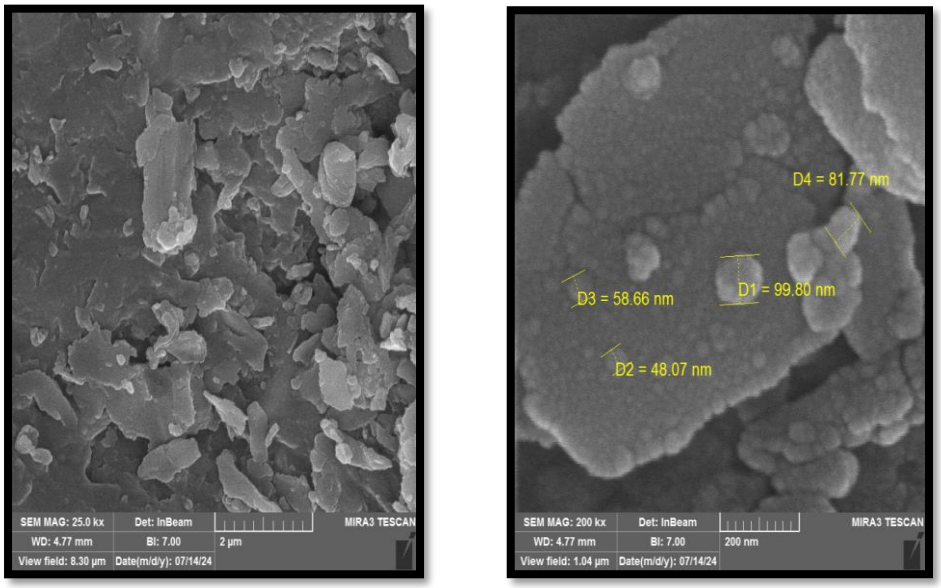

Figure 10. SEM picture of the low-carbon steel (SS41) surface before immersion in a corrosion solution.

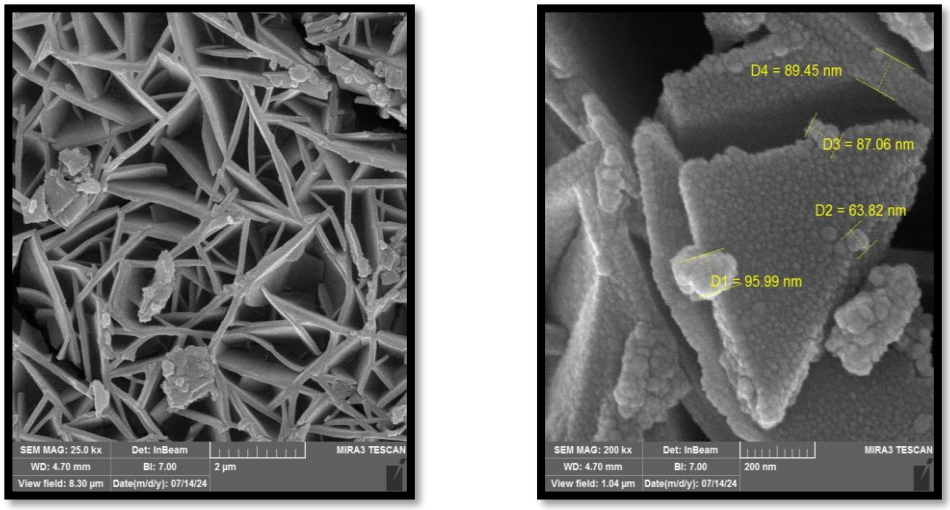

Figure 11. SEM images of the low-carbon steel (SS41) surface after immersion in a corrosion solution (0.5M H_2SO_4) for (3h) at (55℃).

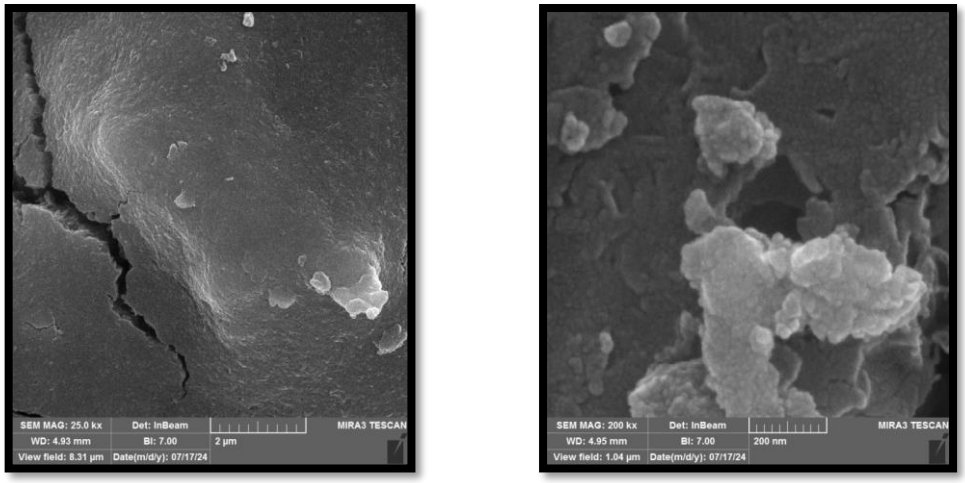

Figure 12. SEM images of the low-carbon steel (SS41) surface after immersion in presence of inhibitor 4-(Dimethylamino) benzaldoxime.

4. CONCLUSION

Increasing the temperature accelerates the corrosion of low-carbon steel (SS41) in solution (0.5 M H_2SO_4). (42-amino-5-chloro benzophenoxime) at six concentrations (50, 100, 150, 200, 250, and 300 ppm) efficiently resisted corrosion of low-carbon steel (SS41) in ($0.5MH_2SO_4$) at temperatures (25, 35, 45, and 55) ℃. As organic inhibitor concentrations and temperature rise, so does inhibition efficiency. Adsorption of inhibitor molecules on the surface of low-carbon steel (SS41) occurs through both chemical and physical processes. The adsorption of organic components on the surface of low-carbon steel (SS41), as well as the chemical adsorption of active sites, aid in corrosion prevention. The Langmuir adsorption isotherm was investigated to have a better grasp of the adsorption idea. The stated thermodynamic parameters, together with the negative standard free energy values, indicate that the adsorption process is spontaneous and endothermic, resulting in a reduction in system entropy. At 55°C, the inhibitory concentration of 2-amino-5-chloro benzophenoxime (300ppm) demonstrated the highest inhibition efficiency (87.77%). The corrosion of low-carbon steel (SS41) in ($0.5MH_2O_4$) is depicted in the image SEM stop it through inhibitor surface adsorption.

ACKNOWLEDGEMENTS

I am profoundly grateful to **Allah** for his guidance and strength throughout this journey. My deepest gratitude goes to my supervisors, Prof. Dr. Ahmed Najm Abd and **Assistant Prof. Dr. Luma Salman Abd**, for their invaluable guidance, encouragement, and constant support. I also extend my thanks to the **Dean**, the **Head**, and the **Staff** of the **Chemistry Department, College of Science, and University of Diyala** for providing a supportive environment.

REFERENCES

[1] A.Thakur, A. Kumar, "Sustainable inhibitors for corrosion mitigation in aggressive corrosive media: a comprehensive study", Journal of Bio-and Tribo-Corrosion, 7, 1-48, 2021, DOI: https://doi.org/10.1007/s40735-021-00501-y?urlappend=%3Futm_source%3Dresearchgate.net%26utm_medium%3Darticle

[2] B. Tuli, "CORROSION: TYPES, THEORIES AND PREVENTIVE MEASURE", I-Manager's Journal on Material Science, 10(4), 2023, DOI: https://doi.org/10.26634/jms.10.4.19303

[3] A. K. Singh, A. K. Singh, D' Silva, "Microbially induced corrosion and its mitigation", Springer Singapore, Indian Institute of technology, Rookee, India, 2020, DOI: https://doi.org/10.1007/978-981-15-8019-2

[4] A. Khadijah, R. Felaly, "Date Seed Extract as Green Corrosion Inhibitor for Steel in Hydrochloric Medium, Jordanian Journal of Engineering & Chemical Industries", 6(1), 2023, DOI: https://doi.org/10.48103/jjeci622023

[5] D. S. Chauhan, C. Verma, M. A. Quraishi, "Molecular structural aspects of organic corrosion inhibitors: Experimental and computational insights", Journal of Molecular Structure, 1227, 129374, 2021, DOI: https://doi.org/10.1016/j.molstruc.2020.129374

[6] H. Assad, A. Kumar, "Understanding functional group effect on corrosion inhibition efficiency of selected organic compounds", Journal of Molecular Liquids, 344, 117755, 2021, DOI: https://doi.org/10.1016/j.molliq.2021.117755

[7] U. Sayin, H. Yuksel, A. Ozmen, M. Birey, "CW-EPR study of 2, 2, 4, 4-tetramethyl-3-pentanone oxime single crystals", Radiation Physics and Chemistry, 79(12), 1220-1224, 2010, DOI: https://doi.org/10.1016/j.radphyschem.2010.07.051

[8] H. M. Jiang, Y. L. Zhao, Q. Sun, X. H. Ouyang, J. H. Li, "Recent advances in NO bond cleavage of oximes and hydroxylamines to construct N-heterocycle", Molecules, 28(4), 1775, 2023, DOI: https://doi.org/10.3390/molecules28041775

[9] S. Wang, "Insights into dynamic covalent chemistry for bioconjugation applications", Doctoral dissertation, Acta Universitatis Upsaliensis, 2017.

[10] W. A. Isa, and Z. W. Ahmed, "Corrosion inhibition of aluminum in acidic medium using amino acid (methionine)", Ibn AlHaitham Journal For Pure and Applied Science, 28(3), pp. 86-102, 2015

[11] A. Kalla, M. Benahmed, N. Djeddi, S. Akkal, and H. Laouer, "Corrosion inhibition of carbon steel in $1M\ H2SO4$ solution by Thapsia villosa extracts", Int J Ind Chem , 7, 419 – 429, 2016, DOI: https://doi.org/10.1007/S40090-016-0094-8

[12] A. M. Preetha, F. R. Selvarani, "Corrosion inhibition of mild steel using aloe barbedens is miller skin extract in 0.5 M HCL", Int. J. Adv. Res, 5, 1457-1467, 2017, DOI: https://doi.org/10.21474/IJAR01/3653

[13] G. I. Udom, G. A. Cookey, and A. A. Abia, "The Effect of acanthus montanus leaves extract on corrosion of aluminium in hydrochloric acid medium", Current Journal of Applied Science and Technology, 25, 1- 11, 2017

[14] P. S. Desai, "Calotropis gigantea leaves ark used as corrosion inhibitor for aluminium in hydrochloric acid", Der Pharma Chemica, 10, 7-12, 2018

[15] C. M. Anbarasi, S. Rajendran, "Surface Protection of Carbon Steel by Hexane sulphonic Acid-Zinc Ion System", ISRN Corrosion, 2014

[16] B. Wang, M. Du, J. Zhang, and C. J. Gao, "Electrochemical and Surface Analysis Studies on Corrosion Inhibition of Q235 Steel by Imidazole Derivative Against CO2 Corrosion", Corrosion Science, 53(1), 353-361, 2011